~~Pergamon Encyclopedia of the Environment~~
"Concise Encyclopedia of Environmental Systems" Ed. P. Young, Pergamon 1993

S

Scale Invariance and Multifractals in the Atmosphere

Scale invariance is a symmetry principle in which the small- and large-scale properties of a system are related by a scale changing operation involving only the scale ratio. Between the corresponding "inner" and "outer" scales, the system has no characteristic size. Multifractals are the scale invariant measures generally obtained when the inner scale of such systems goes to zero. They provide natural descriptions of many nonlinear dynamical systems ranging from phase space portraits of chaotic attractors (Berger *et al.* 1987, Schuster 1988), to velocity and other fields associated with turbulent cascades. In the atmosphere, the governing dynamical equations have no characteristic length from the outer planetary scale down to an inner viscous scale of the order of millimeters. Furthermore, the variability (intermittency) is due to cascade processes in which the large scale modulates the transfer of energy and other conserved fluxes to smaller scales. This phenomenology provides the theoretical basis for multifractal models of the atmosphere. There is also considerable evidence that various atmospheric fields including cloud, rain, temperature, wind and radiation fields are multifractal although the exact range of scales over which this is true is still not clear, and is the subject of ongoing research.

1. Discussion

A basic feature of geophysical systems in general, and of the atmosphere in particular is their extreme variability which involves the appearance of complex (fractal) structures over wide ranges of scale, and which raises immediate problems of description, measurement and modelling. This complexity prompted Richardson (who is best known as the father of numerical weather prediction) to ask in 1926, "Does the wind have a velocity?" (are the trajectories of air particles smooth enough for derivatives to exist?). Pursuing this idea, Richardson proposed that the variability in the atmosphere arises through a series of scale-invariant cascade steps in which the energy flux from solar heating at large scales is redistributed over smaller and smaller scales by the nonlinear dynamics (see Fig. 1 for a modern model). This cascade idea is the basis of Kolmogorov's famous "scaling" (power law) $k^{-5/3}$ spectrum (for the energy in the wind at wavenumber k), and for a series of cascade models (see Monin and Yaglom (1975) for an early review) culminating in the multifractal models described in this article. During roughly the same period as Richardson, and in apparent contrast to the cascades which require a whole series of eddies of decreasing size, Bjerknes and the Norwegian school of meteorology emphasized the importance of a few large structures for forecasting, particularly the "fronts," while Leray and von Neumann in fluid mechanics in the 1930s and 1940s called for a better characterization of the singularities in fluid mechanics. Multifractals, possessing well-defined hierarchies of singularities—a few of which can "dominate" the rest—are the natural framework for studying these issues.

2. Sets, Fractals, Geometry

The simplest illustration of scaling and scale invariance is to consider the geometric idea of the dimension of a set of points. The notion of interest here is that which relates the number of points in the set to its size. The intuitive (and essentially correct) definition of measure dimension that will be used here, is that the number of points $n(L)$ in a (fractal) set S at scale L (e.g., in a sphere of radius L) varies as

$$n(L) \propto L^{d(S)} \tag{1}$$

where $d(S)$ is the dimension of the set. Defining the codimension $C = d - d(S)$ where d is the dimension of space in which the set is embedded, the set is a "fractal" if $C > 0$. A simple example is the number of *in situ* meteorological measuring stations on the earth in a circle radius L (see Fig. 2a). If the measuring stations were uniformly distributed over the surface ($d(S) = 2$), we would obtain $n(L) \propto L^2$, however, the actual distribution (Fig. 2b) is highly nonuniform, empirically yielding $n(L) \propto L^{1.75}$. Alternatively, the density of points is proportional to $L^{d(S)}/L^d = L^{-C}$ which for fractal sets decreases with L; the rate of decrease is characterized by $d(S)$. The fractal dimension of a set (Mandelbrot 1982, Feder 1988) therefore is a measure of its sparseness.

3. Measures, Multifractals, Dynamics

Clouds are not sets, dynamics is not geometry; geophysical systems are usually fields (more generally measures) and their treatment takes us well beyond the geometry of sets, providing us with dynamical "multifractal" generators. Consider a typical empirical data set such as a satellite cloud picture, obtained by a sensor with resolution L where $L_o > L > L_i$, L_o is the outer scale of the variability, and L_i the inner scale. Define the scale ratio $\lambda = L_o/L > 1$ and the field smoothed at scale λ by

$$f_\lambda = \frac{\int_{S_\lambda} f(x)\,dx}{\int_{S_\lambda} dx} \tag{2}$$

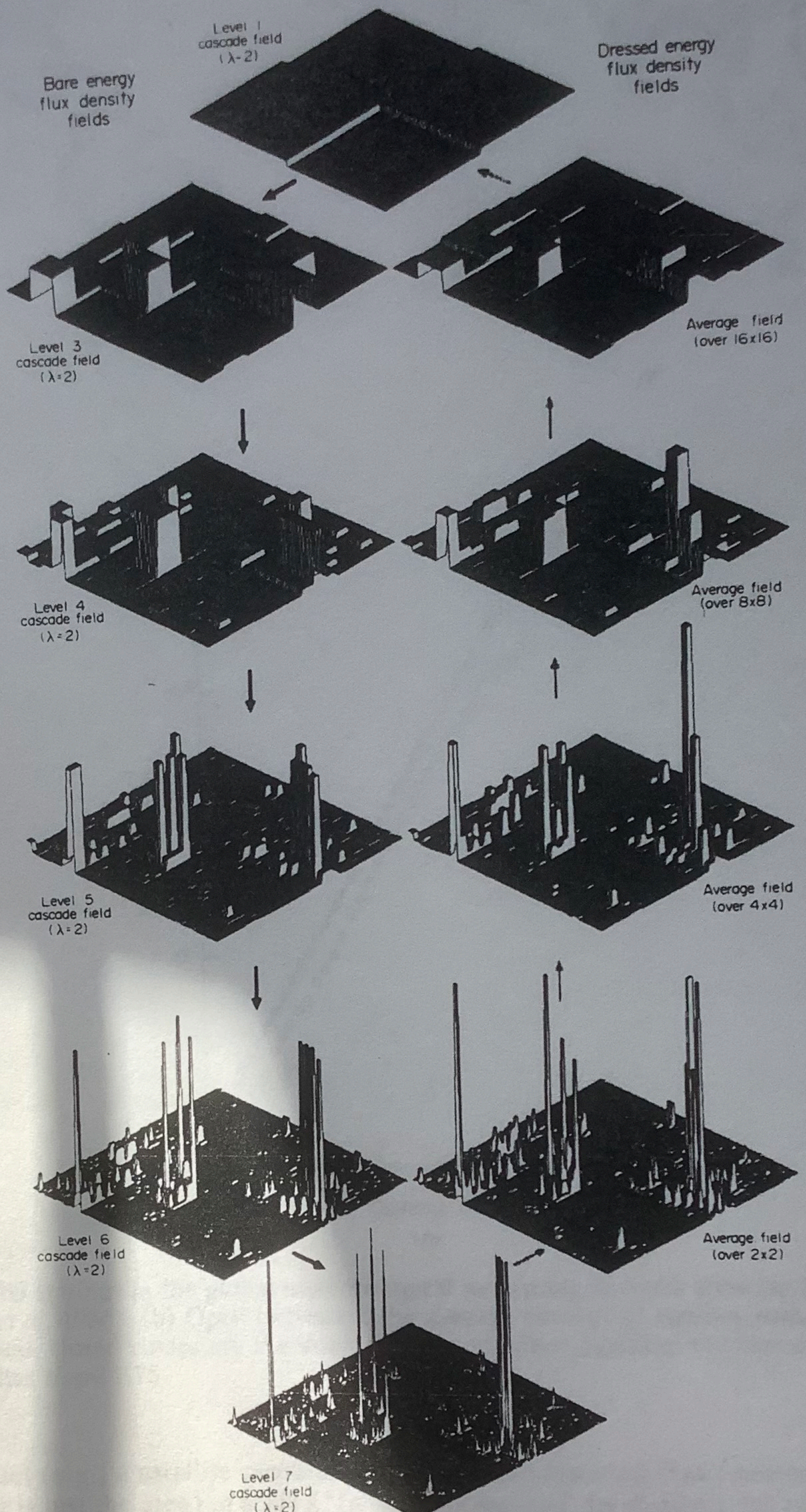

Figure 1
The left-hand side shows the step-by-step construction of a ("bare") multifractal cascade (called an "α model") starting with an initially uniform unit flux density. The vertical axis represents the density of energy (ε) flux to smaller scales which is conserved by the nonlinear terms in the dynamical equations governing fluid turbulence. At each step the horizontal scale is divided by two, and independent random factors are chosen either >1 or <1, normalized to ensure that $\langle\varepsilon\rangle = 1$. The developing spikes are incipient singularities of various orders. The right-hand side shows the effect of smoothing (Eqn. (2)) over larger and larger scales, yielding a "dressed" cascade

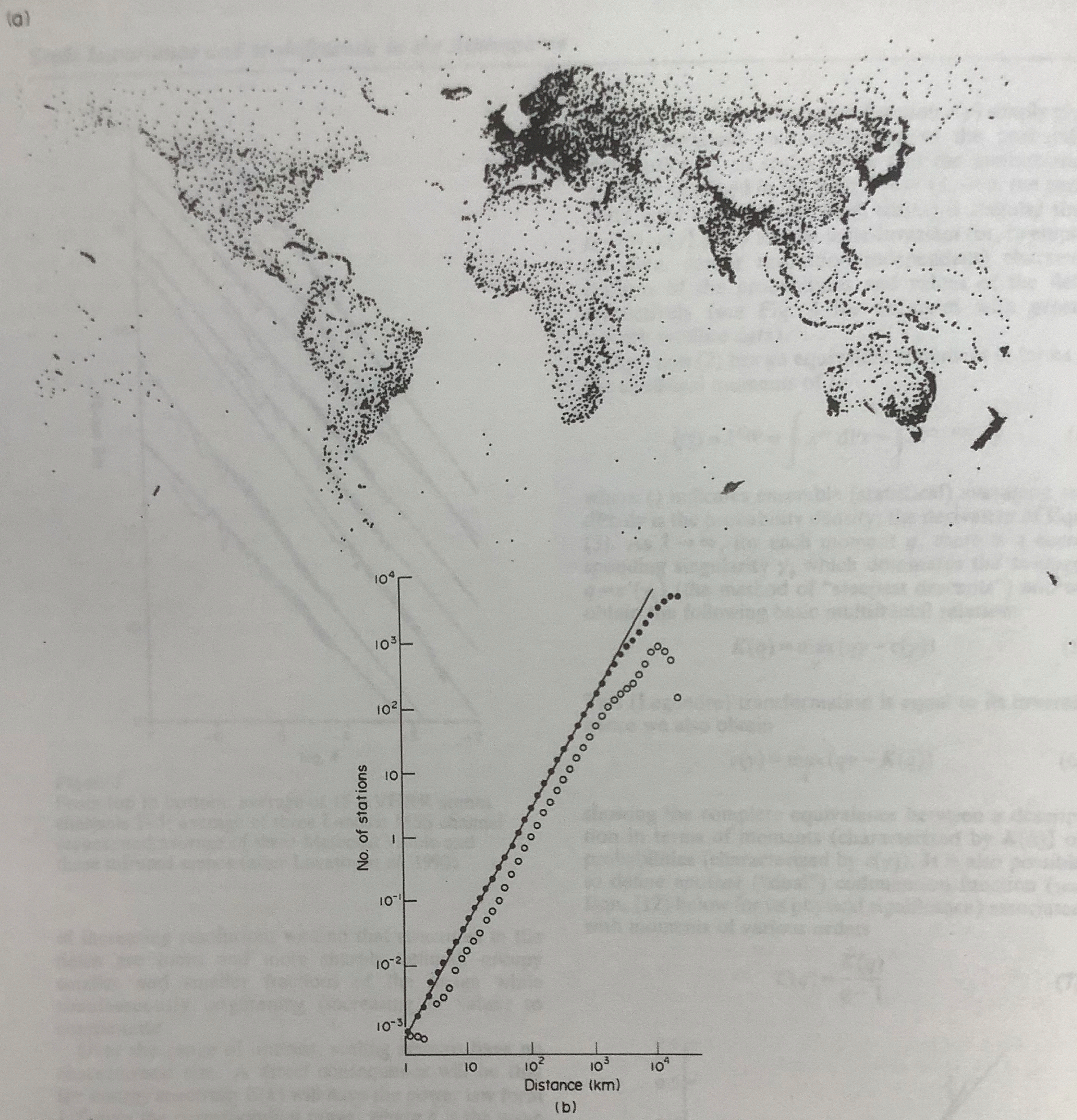

Figure 2
(a) The locations of the 9563 stations in the global meteorological measuring network showing their high degree of sparseness (after Lovejoy *et al.* 1986). (b) Open circles are the average number of stations within annuli of geometrically increasing radii, closed circles are the integral of the previous function, the function $\langle n(L) \rangle$ described in the text. The straight line has slope 1.75

where S_λ is an averaging set (e.g., a satellite resolution element, the denominator is just the area) of scale λ. In the simplest case, called "self-similarity," S_λ is just a reduced copy of the large-scale region S_1 (see Sect. 4 for a discussion of more complex "reductions"). We have also assumed that f has been nondimensionalized (normalized) by dividing the original field by its climatological average value so that the statistical average $\langle f_\lambda \rangle = 1$. As $\lambda \to \infty$, f_λ is an increasingly finer resolution function; if it represents a satellite image with a sensor

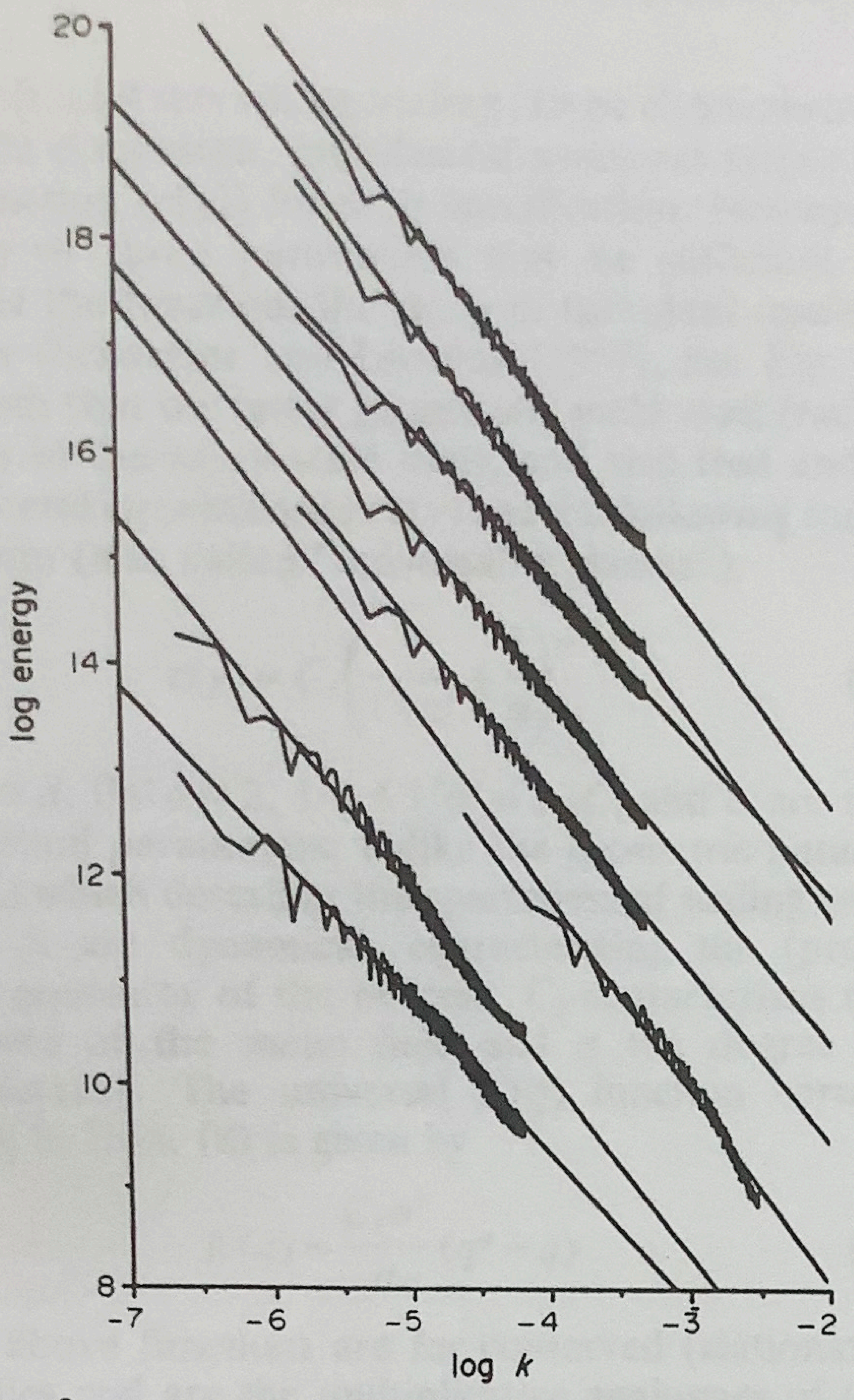

Figure 3
From top to bottom: average of 15 AVHRR scenes channels 1–5; average of three Landsat MSS channel scenes; and average of three Meteosat visible and three infrared scenes (after Lovejoy *et al.* 1993)

of increasing resolution, we find that structures in the fields are more and more sharply defined, occupy smaller and smaller fractions of the image while simultaneously brightening (increasing in value) to compensate.

Over the range of interest, scaling systems have no characteristic size. A direct consequence will be that the energy spectrum $E(k)$ will have the power law form $k^{-\beta}$ over the corresponding range, where k is the wave number and β is the spectral exponent. Figure 3 is a composite showing that such scaling behavior is well respected by cloud radiances at various wavelengths over the range of at least 4000 km to 300 m, with b varying between about 1.4 and 1.9 depending on the wavelength. If we consider how the probability distributions vary with resolution λ, we obtain the following basic multifractal relation:

$$\Pr(f_\lambda > \lambda^\gamma) \approx \lambda^{-c(\gamma)} \qquad (3)$$

where Pr indicates probability, γ is the order of the singularity associated with the "pixel" value f_λ, and $c(\gamma)$ is the associated "codimension." The '$\approx$' sign indicates equality to within factors dependent on the logarithm of λ. Eqn. (3) expresses the fundamental property of a multifractal: the codimension function $c(\gamma)$ simply gives a scale-invariant characterization of the probability distribution at all scales. Note that the mathematical measure obtained in the limit $\lambda \to \infty$ ($L_i \to 0$, the variability goes to arbitrarily small scales) is singular since $f_\lambda \to \infty$. $c(\gamma)$ and γ are the scale-invariant (or, in empirical data, sensor resolution independent) characterizations of the probabilities and values of the field, respectively (see Fig. 4 for examples with geostationary satellite data).

Equation (2) has an equivalent statement in terms of the statistical moments of f_λ:

$$\langle f_\lambda^q \rangle = \lambda^{K(q)} = \int \lambda^{q\gamma}\, \mathrm{dPr} \approx \int \lambda^{q\gamma - c(\gamma)}\, \mathrm{d}\gamma \qquad (4)$$

where $\langle\rangle$ indicates ensemble (statistical) averaging and $\mathrm{dPr}/\mathrm{d}\gamma$ is the probability density, the derivative of Eqn. (3). As $\lambda \to \infty$, for each moment q, there is a corresponding singularity γ_q which dominates the average: $q = c'(\gamma_q)$ (the method of "steepest descents") and we obtain the following basic multifractal relation:

$$K(q) = \max_\gamma (q\gamma - c(\gamma)) \qquad (5)$$

This (Legendre) transformation is equal to its inverse, hence we also obtain

$$c(\gamma) = \max_q (q\gamma - K(q)) \qquad (6)$$

showing the complete equivalence between a description in terms of moments (characterized by $K(h)$) or probabilities (characterized by $c(\gamma)$). It is also possible to define another ("dual") codimension function (see Eqn. (12) below for its physical significance) associated with moments of various orders

$$C(q) = \frac{K(q)}{q-1} \qquad (7)$$

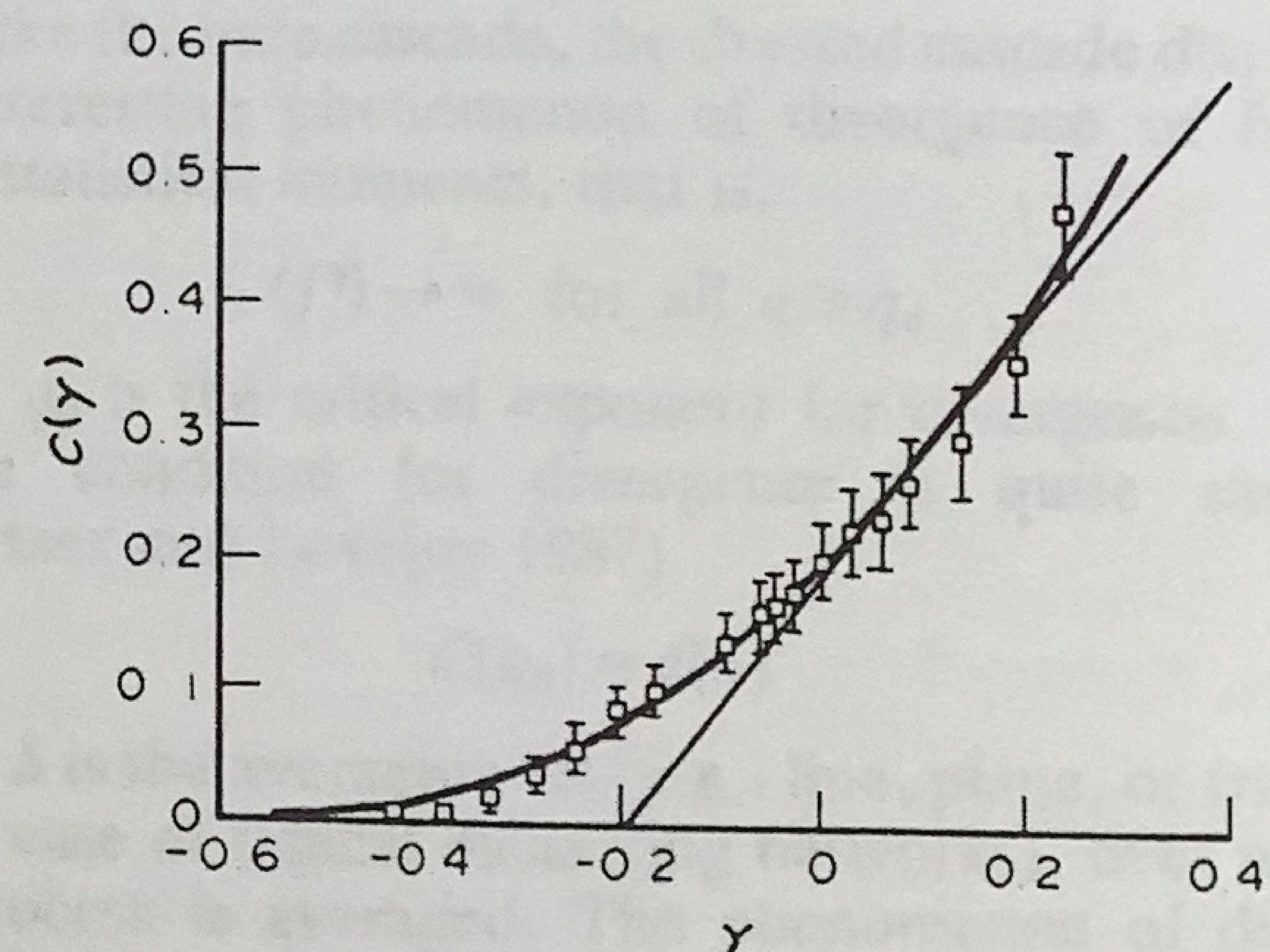

Figure 4
(a) Estimates of the function $c(\gamma)$ obtained from five infrared satellite images with resolution 8 km over an area 1024×1024 km. The points indicate the mean of the six individual $c(\gamma)$ functions obtained at 8, 16, 32, 64, 128, 256 km. The solid curved line is the best fit regression to the universal form and yields α

Unlike fractal sets whose scaling can be characterized by a single dimension, multifractal measures require a whole function ($c(\gamma)$) for their specification. However, only two or three parameters may be sufficient to determine the function: the study of turbulent cascade processes (Schertzer and Lovejoy (1987), see Fig. 1) shows both that the latter generically yield multifractal measures in the small-scale limit, and also that under fairly general circumstances $c(\gamma)$ has the following functional form (also called "universality classes"):

$$c(\gamma) = C_1\left(\frac{\gamma}{C_1\alpha'} + \frac{1}{\alpha}\right)^{\alpha'} \qquad (8)$$

with $C_1 \leq d$, $0 \leq \alpha \leq 2$, $1/\alpha + 1/\alpha' = 1$. C_1 and α are the fundamental parameters: unlike the geometric parameter $d(S)$ which describes the sparseness of scaling sets, C_1 and α are dynamical, characterizing the (probability) generator of the process. C_1 characterizes the sparseness of the mean field and α the degree of multifractality. The universal $K(q)$ function corresponding to Eqn. (8) is given by

$$K(q) = \frac{C_1\alpha'}{\alpha}(q^{\alpha} - q) \qquad (9)$$

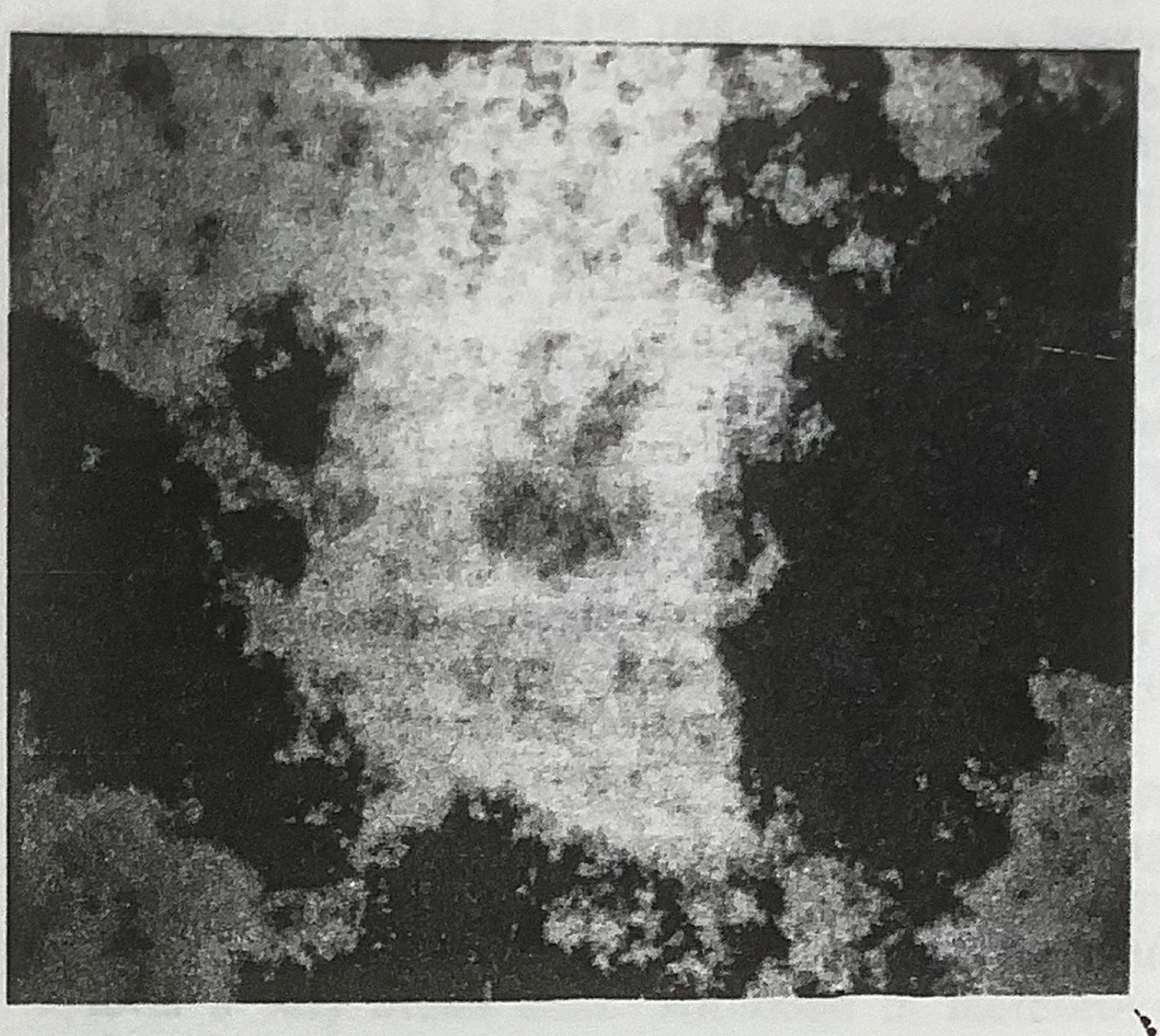

Figure 5
Multifractal passive scalar cloud from a continuous cascade process with $\alpha = 1.6$, on a 512×512 point grid (after Schertzer and Lovejoy (1991) in collaboration with Jean Wilson, Gadje Sarma)

The above functions are for conserved (stationary) quantities and are the multiplicative analogues of the standard central limit theorem for the addition of random variables. When $\alpha = 2$, the multifractals defined by Eqns. (3, 8) have lognormal probabilities, that is, the logarithm has a Gaussian distribution (see, however, the caveat below about "dressed" quantities), so that the multifractal nature of the atmosphere can be consistent with a lognormal phenomenology (if α is nearly 2), or a monofractal phenomenology (a single fractal dimension) when $\alpha \simeq 0$. Empirical values of α reported in the literature (see especially Schmitt *et al.* 1992) include $\alpha \simeq 1.3$, 1.45 (wind speed, in wind tunnel and atmosphere respectively), $\alpha \simeq 1.2$ (temperature) and $\alpha \simeq 1.35$ (rain and visible cloud radiances). For other quantities, related to these by either dimensional and/or power law relations, the corresponding $c(\gamma)$ functions can be obtained by the linear transformation $\gamma \rightarrow a\gamma - H$. For example in turbulent cascades, the energy flux ε is conserved, and fluctuations in components of the velocity field are obtained by $\Delta v = \varepsilon^{1/3}\lambda^{-1/3}$ hence $a = H = 1/3$. Varying H changes the spectral exponent and hence the smoothness. For passive scalar clouds (see Fig. 5 for an illustration), the corresponding quantities are $\Delta\rho = \varphi^{1/3}\lambda^{-1/3}$ where $\varphi = \chi^{3/2}\varepsilon^{-1/2}$ and χ is the variance flux of the passive scalar concentration ρ.

Before turning to the problem of anisotropy, we must first discuss a complication which arises because of a basic distinction between "bare" and "dressed" multifractal properties. The "bare" properties are essentially theoretical: they are typically obtained after a cascade process has proceeded only over a finite range of scales (see the left-hand side of Fig. 1); strictly speaking, Eqns. (8–9) apply only to these quantities. The experimentally accessible quantities are different; they are obtained by integrating cascades (e.g., with a measuring device) over scales much larger than the inner scale of the cascade (which in the atmosphere is typically of the order of 1 mm). The properties of such spatial (and/or) temporal averages are approximated by those of the "dressed" cascades, that is, those in which the cascade has proceeded down to the small-scale limit and then integrated over a finite scale (see the right-hand side of Fig. 1). The small-scale limit of these multiplicative processes is singular and is reponsible for this basic distinction.

Unlike the bare cascade, the dressed cascade displays the interesting phenomenon of divergence of high-order statistical moments, that is,

$$\langle f^q \rangle \rightarrow \infty \text{ for all } q \geq q_d \qquad (10)$$

where q_d is the critical exponent for divergence. The precise condition for divergence is quite simple (Schertzer and Lovejoy 1987)

$$C(q_d) = d(S) \qquad (11)$$

where S is the averaging set (e.g., line, plane, or fractal in the case of typical measuring networks), over whch the process is averaged. The phenomenon of divergence of high-order statistical moments arises directly from the fact that $C(q)$ is often unbounded (see Eqns. (7, 9)), and hence for large enough q, $C(q) > d(S)$. Conversely for a fixed q, divergence will still occur if the set S is sufficiently sparse so that $d(S)$ is small enough. The dressed codimension function is the same as that of the bare function for $\gamma < \gamma_d$ where $c'(\gamma_d) = q_d$. For $\gamma > \gamma_d$, it is a straightline, slope q_d. Empirical values of q_d include 5, 5, 1.7 for wind, temperature, and rain, respectively (see Lovejoy and Schertzer (1986) for a review). In empirical data sets this implies that moments increase with sample size; troublesome "outliers" continue to exist even when the latter is enormous.

A formal analogy can be established between multifractals and thermodynamics: $c(\gamma)$ is the analogue of the entropy, $C(q)$ is the analogue of the free energy and q is the inverse temperature. Using this analogy, the qualitative change in behavior associated with the divergence of moments can be considered to be a multifractal phase transition.

4. *Self-Similarity, Self-Affinity, Generalized Scale Invariance*

The example of scaling in fluid turbulence where isotropic scaling ideas have been developed over a considerable period of time has been considered so far. However, the atmosphere is not a simple fluid system, nor is it isotropic; gravity leads to differential stratification, and the rotation of the earth to the Coriolis force and to differential rotation; radiative and microphysical processes lead to further complications. However, even when the exact dynamical equations are unknown (as is generally the case in geophysics), it can still be argued that at least over certain ranges, these phenomena are likely to be symmetric with respect to scale changing operations. This view is all the more plausible when it is realized that the requisite scale changes needed in Eqn. (2) to transform the large-scale S_1 to the small-scale S_λ can be very general.

To see this, introduce a scale-changing operator $\mathbf{T}_\lambda$ defined by: $\mathbf{T}_\lambda S_1 = S_\lambda$. "Self-similar" measures will satisfy Eqn. (3) with $\mathbf{T}_\lambda = \lambda^{-1} = \lambda^{-1}\mathbf{I}$ where $\mathbf{I}$ is the identity matrix, that is, $\mathbf{T}_\lambda$ is a simple reduction by factor λ. However, much more general scaling transformations are possible; detailed analysis shows that practically the only restriction on $\mathbf{T}_\lambda$ is that it has (semi-) group properties: $\mathbf{T}_\lambda = \lambda^{-\mathbf{G}}$ where $\mathbf{G}$ is the generator of the group of scale changing operations (this formalism is called "generalized scale invariance" or GSI, Schertzer and Lovejoy (1987)). For example, "self-affine" measures involve reductions coupled with compression along one (or more) axes; $\mathbf{G}$ is again a diagonal matrix but with not all diagonal elements equal to one. If $\mathbf{G}$ is still a matrix ("linear GSI") but has off-diagonal elements, then $\mathbf{T}_\lambda$ might compress an initial circle S_1 into an ellipsoid as well as rotate the result yielding, for example, cloud texture and morphology. Linear and nonlinear GSI (where $\mathbf{G}$ can vary even randomly from place to place) has already been used to model galaxies and clouds (for a review, see Schertzer and Lovejoy (1989)). Empirically, the trace of $\mathbf{G}$ (called the "elliptical dimension" d_{el} of the system) has been estimated in both rain and wind fields to have the values 2.22 and 2.55, respectively, indicating that the fields are neither isotropic ($d_{el}=3$), nor completely stratified ($d_{el}=2$), but are rather in between, becoming more and more stratified at larger and larger scales.

GSI is also important for dynamical (space–time) multifractal processes; $\mathbf{G}$ then determines the appropriate space–time transformation which specifies the lifetimes of processes as functions of their size. In turbulence and meteorology, this can be regarded as a generalization of Taylor's hypothesis of "frozen turbulence." Knowledge of $\mathbf{G}$, C_1, α and $\mathbf{H}$ can then be used to perform dynamical multifractal simulations. It also provides the basis for multifractal forecasting which systematically exploits the "stochastic memory" of the atmosphere to predict the future behavior from time history information.

Defined by both the function $c(\gamma)$ (or equivalently, by the probability generator), and the scale changing generator $\mathbf{G}$, anisotropic multifractals display a tremendous variety of behavior: scaling systems therefore form a very broad class. Although in meteorology, there are good theoretical reasons to expect multifractal behavior, these systems are just beginning to be explored and there is no consensus about the exact limits. Systematic multifractal analysis of atmospheric fields as well as their numerical simulation (which produces surprising multifractal images, see Fig. 4), undoubtedly helps us understand atmospheric dynamics, predictability and its limits, as well as contribute towards quantitative uses of remotely sensed and *in situ* data.

See also: Catastrophe Theory; Chaos Theory; *Chaotic Dynamics*; Earth–Atmosphere System: Identification of Optical Parameters; *Fractals*; Laser Spectroscopy in Atmospheric Analysis; Remote Sensing and Image Processing Methods in Geology; *Transport Processes in Heterogeneous Materials: Theory and Measurement*

Bibliography

Berger P, Pomeau Y, Vidal C 1987 *Order Within Chaos*. Wiley, New York

Feder J 1988 *Fractals*. Plenum, New York

Lovejoy S, Schertzer D 1986 Scale invariance, symmetries fractals and stochastic simulation of atmospheric phenomena. *Bull. Am. Meterol. Soc.* **67**, 21–32

Lovejoy S, Schertzer D, Ladoy P 1986 Fractal characterisation of inhomogeneous measuring networks. *Nature* **319**, 43–4

Lovejoy S, Schertzer D, Silas P, Tessier Y, Lovallée D 1993 The unified scaling model of atmospheric dynamics and systematic analysis of scale invariance in cloud radiances. *Ann. Geophys.* **11**, 119–27

Mandelbrot B 1982 *The Fractal Geometry of Nature*. Freeman, San Francisco, CA

Monin A S, Yaglom A M 1975 *Statistical Hydrodynamics*, Vols. 1, 2. MIT Press, Cambridge, MA

Schertzer D, Lovejoy S 1987 Physically based rain and cloud modeling by anisotropic, multiplicative tubulent cascades. *J. Geophys. Res.* **92**, 9693–714

Schertzer D, Lovejoy S 1989 Generalized scale invariance and multiplicative processes in the atmosphere. *Pageoph* **130**, 57–81

Schertzer D, Lovejoy S 1991 *Scaling, Fractals and Nonlinear Variability in Geophysics*, Vol. 1. Kluwer, Dordrecht, The Netherlands

Schmitt F, Lavallée D, Schertzer D, Lovejoy S 1992 Empirical determination of universal multifractal exponents in turbulent velocity fields. *Phys. Rev. Lett.* **68**, 305–8

Schuster H G 1988 *Deterministic Chaos*. VCH, Weinheim, Germany

S. Lovejoy
[McGill University, Montreal, Canada]

D. Schertzer
[Université Pierre et Marie Curie, Paris, France]

Seasonal Adjustment

The effect of a natural seasonal cycle present in an environmental time series is conventionally discounted by comparing variations with the long-term average for the relevant time of the year, and the seasonal pattern itself is seldom closely studied. This is unfortunate; estimation and subtraction of the seasonal cycle, if carried out correctly, allows for inspection of the pattern and removes the seasonality with minimum distortion of the nonseasonal variations. In this article, it is shown that the seasonal pattern in a series may be constructed by recursive fixed-interval smoothing estimation of a dynamic harmonic regression time-series model incorporating seasonality. The effectiveness of this seasonal adjustment technique is illustrated by applying it to a record of atmospheric carbon dioxide concentration. This reveals some subtle influences that are not obvious in the original series.

1. Background

It is, perhaps, paradoxical that, although seasons are essentially environmental phenomena, seasonal adjustment is a practice more usually associated with socio-economic time series. It is unfortunate that climatic records are seldom discussed in seasonally adjusted terms, not only because it is a convenient and efficient means of removing seasonal influences, but also because it involves the construction of the seasonal variations themselves. In general, natural seasonal variations have received little attention, presumably because they are assumed to be highly regular and fully understood. However, as the example presented below will show, even the slight changes of seasonal pattern that do occur may be of great interest.

The method of seasonal adjustment described here is a specific application of recursive fixed-interval smoothing algorithms described in other articles (see *Extrapolation, Interpolation and Smoothing of Nonstationary Time Series*; *Spectral Analysis, Time-Variable*).

2. A Model for Seasonal Time Series

The seasonal time series are considered to be represented by the component model (see Young and Young 1992; *Component (Structural) Models of Time Series*)

$$y(k) = t(k) + p(k) + \xi(k) \qquad (1a)$$

where $t(k)$ is a low-frequency "trend" component; $p(k)$ is a time-variable-parameter harmonic regression (or dynamic harmonic regression, DHR) component of the form

$$p(k) = \sum_{i=1}^{i=F} a_{1i}(k)\cos(2\pi f_i k) + a_{2i}(k)\sin(2\pi f_i k) \qquad (1b)$$

and $\xi(k)$ represents an "irregular" component, that is, that part of $y(k)$ not modelled by $t(k)$ and $p(k)$. If the seasonal component can be represented by the sum of harmonic components, then $p_1 = 1/f_1$ will represent the fundamental period, and $p_i = 1/f_i$, $i = 1, 2, \ldots, F$, will be associated with the harmonic periods (e.g., for an annual cycle with monthly data the fundamental period $p_1 = 12$ months and the harmonic periods are $p_2 = 6$, $p_3 = 4$, $p_4 = 3$, $p_5 = 2.4$, $p_6 = 2$ months, with p_6 representing the component at the Nyquist frequency of 0.5 cycle/sample).

Distinction between the various components in Eqn. (1b) is made according to their frequency. This is most straightforward in the case of stationary time series; that is, a series with no trend and a constant seasonal pattern. In this case, the mean is represented by spectral power at zero frequency, and the spectral representation of the seasonality consists of discrete spikes at each of the harmonic frequencies. The irregular component consists of variation of the remaining frequencies. Introducing time variability of the mean level and seasonality means that a range of frequencies becomes associated with each component. The more rapidly these components vary, the wider their frequency bands become.

It is unlikely that seasonality and especially trend components will arise from any simple, readily identifiable factor, and spectral analysis of seasonal time series seldom reveals sharply distinct features associated with the various components. It is, therefore, inevitable that the width of the frequency band representing each component has to be judgementally determined.

3. Estimating the Components of the Seasonal Model

Only the trend and seasonal components are usually explicitly estimated, the irregular component being obtained by residual. Seasonal adjustment of the original series is achieved by subtracting the seasonal component alone.

In the example discussed later, the parameters for the time-varying trend and each of the harmonic components of the seasonal pattern are estimated sepa-